ORIGINAL RESEARCH

Anticipation and Verification of Dendrobium-Derived Nanovesicles for Skin Wound Healing Targets, Predicated Upon Immune Infiltration and Senescence

Jin Tu[1–3],*, Feng Jiang[4],*, Jieni Fang[2], Luhua Xu[2], Zhicong Zeng[2], Xuanyue Zhang[1], Li Ba[1], Hanjiao Liu[1,3], Fengxia Lin [2]

[1]Department of Nursing, Seventh Clinical Medical College, Guangzhou University of Chinese Medicine, Shenzhen, Guangdong, 518100, People's Republic of China; [2]Department of Cardiovascular, Shenzhen Bao'an Traditional Chinese Medicine Hospital, Guangzhou University of Chinese Medicine, Shenzhen, Guangdong, 518100, People's Republic of China; [3]Department of Nursing, Shenzhen Hospital of Integrated Traditional Chinese and Western Medicine, Shenzhen, Guangdong, 518100, People's Republic of China; [4]School of Traditional Chinese Medicine, Beijing University of Chinese Medicine, Beijing, 102488, People's Republic of China

*These authors contributed equally to this work

Correspondence: Fengxia Lin, Department of Cardiovascular, Shenzhen Bao'an Traditional Chinese Medicine Hospital, Guangzhou University of Chinese Medicine, Shenzhen, Guangdong, 518100, People's Republic of China, Email szlinfx@163.com; Hanjiao Liu, Shenzhen Hospital of Integrated Traditional Chinese and Western Medicine, Shenzhen, Guangdong, 518100, People's Republic of China, Email liuhanjiao000@163.com

Background: *Dendrobium*, with profound botanical importance, reveals a rich composition of bioactive compounds, including polysaccharides, flavonoids, alkaloids, and diverse amino acids, holding promise for skin regeneration. However, the precise mechanism remains elusive. Seeking a potent natural remedy for wound healing, exocyst vesicles were successfully isolated from *Dendrobium*.

Aims of the Study: This investigation aimed to employ bioinformatics and in vivo experiments to elucidate target genes of *Dendrobium*-derived nanovesicles in skin wound healing, focusing on immune infiltration and senescence characteristics.

Materials and Methods: C57 mice experienced facilitated wound healing through *Dendrobium*-derived nanovesicles (DDNVs). Bioinformatics analysis and GEO database mining identified crucial genes by intersecting immune-related, senescence-related, and PANoptosis-associated genes. The identified genes underwent in vivo validation.

Results: DDNVs remarkably accelerated skin wound healing in C57 mice. Bioinformatics analysis revealed abnormal expression patterns of immune-related, senescence-related, and pan-apoptosis-related genes, highlighting an overexpressed IL-1β and down-regulated IL-18 in the model group, Exploration of signaling pathways included IL-17, NF-kappa B, NOD-like receptor, and Toll-like receptor pathways. In vivo experiments confirmed DDNVs' efficacy in suppressing IL-1β expression, enhancing wound healing.

Conclusion: Plant-derived nanovesicles (PDNV) emerged as a natural, reliable, and productive approach to wound healing. DDNVs uptake by mouse skin tissues, labeled with a fluorescent dye, led to enhanced wound healing in C57 mice. Notably, IL-1β over-expression in immune cells and genes played a key role. DDNVs intervention effectively suppressed IL-1β expression, accelerating skin wound tissue repair.

Keywords: plant-derived nanovesicles, *Dendrobium*, immune infiltration factors, cellular aging, skin injury recovery

Introduction

The skin, as a natural defense mechanism, faces challenges from acute injuries and diseases globally.[1] Approximately 1 billion individuals globally are afflicted by acute and chronic wounds.[2–4] Wound management expenses account for up to 3% of healthcare expenditures in developed nations. The delayed healing of acute wounds can lead to the progression of chronic wounds, resulting in an annual cost of approximately $50 billion for managing chronic wounds in the United States alone,[5] Despite the availability of a broader array of wound treatments, achieving the desired outcome remains challenging, imposing

a substantial economic and social burden on the global healthcare system,[4,6] Promoting skin wound healing and preventing chronic wounds are major clinical challenges today.

Dendrobium officinale Kimura et Migo, an essential epiphyte belonging to the *Orchidaceae* family, holds a distinguished status as a traditional Chinese medicinal herb with a history spanning thousands of years. The polysaccharides, alkaloids, and flavonoids extracted from *Dendrobium* are regarded as the principal bioactive components of this medicinal herb[7–10] with anti-inflammatory, immunomodulatory,[9] anti-cancer, neuroprotective[11] and antioxidant activities.[12] *Dendrobium nobile* polysaccharide plays a crucial role in shielding skin fibroblasts from UVA-induced photoaging[13] and regulating immune cells to mitigate skin inflammation.[14] While recognized for cosmetic benefits,[15–19] Although some studies have explored the potential of *Dendrobium ironum* for skin repair, there remains a scarcity of specific research regarding its role in promoting wound healing. This knowledge gap highlights the need for further research to unravel the potential of *Dendrobium* as a wound healing-promoting medicine.

Exosomes, crucial in wound healing,[20] regulate immune cells,[21–23] endothelial cells[24,25] and skin fibroblasts[26,27] across different phases. However, exosomes derived from animals pose challenges as they are inherently immunogenic, have limited availability, are difficult to procure, prone to degradation, and entail high storage costs. In contrast, plant-derived exosomes can be obtained in ample quantities, boast low immunogenicity, offer cost-effective solutions, demonstrate remarkable stability, and show consistent quality from batch to batch.[28–30] Contemporary reports suggest the potential of plant-derived nanovesicles, extracted from plants such as ginseng,[31] wheat,[32] grapefruit[6] and Aloe vera,[33] for wound healing applications. In our earlier research, our team successfully isolated and purified exosomes sourced from safflower plants, and our findings conclusively showed that these exosomes exhibit superior modulation of endothelial inflammation compared to safflower extracts. So we attempting to isolate and purify exocysts from Dendrobium plants to delve further into the potential impact of Dendrobium-derived exosomes on wound healing.

Wound healing entails the intricate interplay of various cell types and molecular signals across different skin tissue layers, culminating in a multifaceted biological process.[5,34] The four distinct phases of hemostasis, inflammation, proliferation, and remodeling dynamically unfold in close coordination and interaction.[5] Senescent cell deterioration during improper healing weakens immune response, leading to delayed or failed wound healing;[35,36] During the concluding stage of wound healing, granulation tissue undergoes replacement by scarring, immune cells are released from the epidermis, with some undergoing senescent apoptosis, while others strategically position themselves in the dermis to elicit an immune response and actively participate in wound healing within the peri-wound tissue.[37,38] This process plays a pivotal role in the comprehensive wound repair process. Moreover, it is plausible that DDNVs may have the capacity to regulate apoptosis, immune cell infiltration, and cellular senescence, thereby expediting the wound healing process. Consequently, in this study, our goal is to identify key genes associated with immune infiltration, senescence and pan-apoptosis, and to utilize DDNVs as targeted agents to modulate immune cell infiltration, cellular senescence and apoptosis, and to promote skin tissue repair. Figure 1 depicts the theoretical framework illustrating the regulatory role of DDNVs in promoting the neogenesis and repair of skin tissue.

Method

Animal Experiment Materials and Methods

Materials

DIR (Mackli, D909616, China). SteadyPure Rapid RNA Extraction Kit (AG, 21023, China). Evo M-MLV Mix Kit (AG, 11728, China). Q-PCR Kit (AG, 11701, China). Dewaxing Fluid (Servicebio, G1128, China). HE Dye Kits (Servicebio, G1003, China).

Extraction and Purification of DDNVs

Fresh *dendrobium* was purchased from Huoshan County, Lu'an City, Anhui Province, where it has been identified by Zhao Xinlei, a botanist, as *Orchidaceae, Dendrobium* and is recorded in the Shanghai Chenshan Herbarium (CSH) under the accession barcode: CSH0070204. The use of this plant material for research does not require additional approval under institutional or local regulations. The extraction and purification process of DDNVs involved the following steps:

①Abstracting and washing: Freshly harvested *Dendrobium officinale* in spring underwent three rinses with purified water and drying in a fume hood.
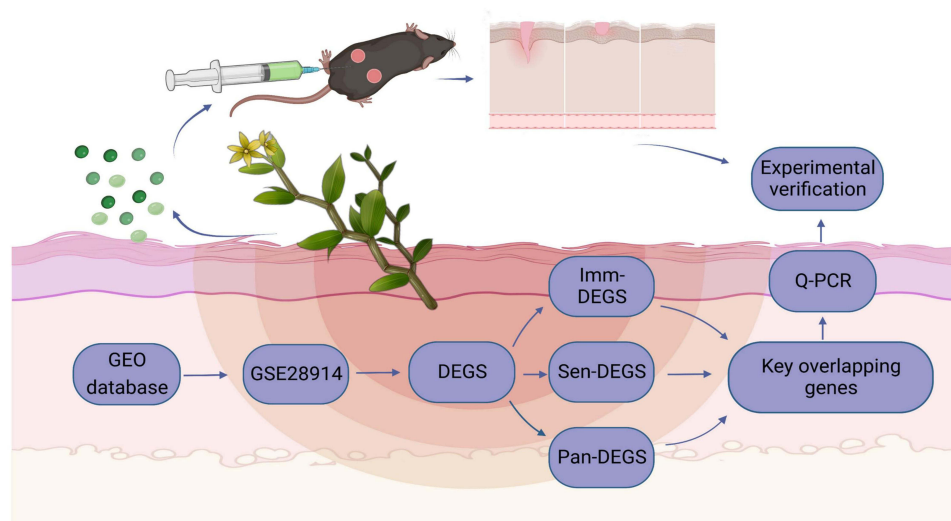
Figure 1 Effectiveness of the DDNVs for skin wound healing program. Image created with BioRender.com, with permission.

②Tissue pulverization: *Dendrobium officinale* was pulverized using a wall-breaking machine (Joyoung, L18-P132, China), soaked in double-distilled water for 3 minutes, and the supernatant was collected.

③Supernatant ultracentrifugation pretreatment: Centrifuge the supernatant at 300g for 10 minutes, then at 2000g for 20 minutes, and finally at 10000g for 30 minutes to obtain the supernatant.

④Ultracentrifugation: After centrifugation at 135,000g for 70 minutes, retain a portion of the supernatant for in vivo experimental control. Discard the remaining supernatant, take the precipitate, and resuspend it in 20 mmol/L Tris-HCl to obtain a green suspension enriched with DDNVs.

⑤Second ultracentrifugation to remove impurities: Centrifuge at 135,000g for 70 minutes, discard the supernatant, take the precipitate, and resuspend it with 20 mmol/L Tris-HCl to obtain a clarified suspension rich in DDNVs.

⑥Four concentrations of sucrose water purification: In the purification process, four sucrose concentrations (15%, 30%, 45%, 60%) were prepared by dissolving sucrose in 20 mmol/L Tris-HCl. The DDNVs, fully resuspended, were gradually added to the uppermost layer of the sucrose gradient to ensure proper stratification. The centrifuge tube, with added concentrations, was gently placed in the center and centrifuged at 150,000g for 3 hours. Post-centrifugation, exosomes were mainly distributed among the 30%, 45%, and 60% sucrose pads. The bottom layer, between the 60% sucrose pads, was aspirated with a 1 mL syringe. The aspirated DDNVs were replenished with 20 mmol/L Tris-HCl to the entire tube, centrifuged at 135,000g for 70 minutes, washed to remove excess sucrose, and finally resuspended with 20 mmol/L Tris-HCl to obtain purified DDNVs.

⑦Filtration: Filter the suspension through a 0.22 um filter cartridge to obtain a sterile DDNV suspension. Simultaneously, filter the DDNVs supernatant through a 0.22um filter to remove bacteria for subsequent experiments. Finally, the protein concentration of the purified DDNVs was determined using a BCA kit.

Transmission Electron Microscopy to Observe the Morphology and Size of DDNVs

For the observation of the structural morphology and size of DDNVs using transmission electron microscopy (TEM), a small droplet of the sample was initially placed on a clean slide. The carrier screen was then gently floated on the drop, allowing the sample to be aspirated for a duration of 2 minutes. Subsequently, any excess sample liquid was carefully blotted up using filter paper, ensuring that only a thin film of the sample liquid remained on the carrier screen. Next, a drop of negative staining solution was placed on the slide, and the undried copper mesh was allowed to float on the droplet. After 2 minutes, the surplus staining solution was blotted up with filter paper, and the slide was allowed to dry naturally. This facilitated the observation of DDNVs using transmission electron microscopy (Tecnai G2 Spirit Twin TEM).

Determination of the Particle Size of DDNVs

To ascertain the particle size of plant nanovesicles, the exosome solution was pre-diluted (Dilution factor:1x10e3). After stabilizing at room temperature, a nanoparticle sizer, Nano Tracking Analysis (NTA), utilizing Nanosight300 (Malvern Instruments, UK), was utilized. The laser irradiated the particles in the sample, and particle size distribution was calculated by observing Brownian motion.

Animals

Male C57BL/6J mice (JW-C57002), aged 6–8 weeks, were acquired from LiaoningChangsheng biotechnology co., Ltd. The mice were housed in a pathogen-free environment, maintaining a standard 12-hour light/dark cycle, and were provided ad libitum access to food. Standard temperature and humidity conditions were upheld. All experiments were approved by the Animal Ethics Committee of Shenzhen Glorybe Biotechnology Co., Ltd, under batch number RW-IACUL-23-0029. The experimental procedures were consistently conducted in strict compliance with the Guidelines for the Use of Laboratory Animals of the National Institutes of Health of the United States of America.

Uptake of DDNVs by Skin Tissues

Male C57BL/6J mice were anesthetized by intraperitoneal injection of 0.3% sodium pentobarbital at 60 mg/kg, and their backs were shaved to prepare for the experiment. Afterwards, 200ul of 20 mmol/L Tris-HCl (used as a negative control) and 200ul of DIR-DDNVs, labeled with a calculated protein concentration of 5 mg/mL, were subcutaneously injected into the dorsal skin using a syringe. DIR, a lipophilic carbocyanate ester recognized for its near-infrared fluorescence, was utilized. It emits a highly bright and stable red fluorescence when incorporated into the film.[39] On the second day, skin tissues were collected, frozen, and cryosectioned to a thickness of 10 um. The samples were then stained with 10 ug/mL DAPI and observed under a fluorescence microscope. Photographs were taken to analyze the fluorescent signals and evaluate the distribution and localization of the labeled DIR-DDNVs within the skin tissues.

Skin Wound Healing Assay

Skin wound models were created on the backs of male C57BL/6J mice by making circular total dermal excision wounds measuring 6 mm in diameter. The mice were then randomly assigned to three treatment groups, each consisting of 5 mice: ①Control group: Received a subcutaneous injection of 200ul 20 mmol/L Tris-HCl each day. ②DDNVs group: Received a subcutaneous injection of 200ul DDNVs (protein concentration of 5mg/mL) each day. ③*Dendrobium* supernatant group: Received a subcutaneous injection of 200ul *Dendrobium* supernatant with *Dendrobium* exosomes removed (protein concentration of 5mg/mL) each day. The subcutaneous injections were administered on day 0, 3, 6, and 10, respectively, following the assigned groups. The wounds were carefully monitored, and their healing progress was weighed and recorded. The wound healing rate was then compared among the three treatment groups to evaluate the potential effect of DDNVs on wound healing.

HE Staining

On day 10 post-injury, tissue samples from both the wound bed and the surrounding healthy skin were collected. These tissue samples were fixed in 4% paraformaldehyde and then dehydrated using a gradient alcohol series. Subsequently, the samples were embedded in paraffin and sliced into 10-μm-thick sections perpendicular to the surface of the wound using a slicer. Following this, the sections underwent HE (hematoxylin and eosin) staining, following the standard staining procedure. Once the staining process was completed, the sections were examined under a microscope, and images were captured and analyzed.

Real-Time Quantitative PCR (Q-PCR) Analysis

To analyze the expression levels of relevant genes in mouse skin tissues after DDNVs intervention, total RNA was extracted from the mouse skin tissues using the Steady Pure Rapid RNA Extraction Kit, following the manufacturer's instructions. After RNA extraction, cDNA synthesis was performed using the Evo M-MLV Mix Kit. For the q-PCR experiments, SYBR® Green Pro Taq HS premixed qPCR reagents were utilized, and the q-PCR reaction cycle was set up using Light cyder 480II,96 (GS000134). To ensure accurate results, the data were normalized using the expression of the β-actin gene as an internal reference gene. The primer sequences used for the q-PCR are provided in Table 1.

Table 1 Primer Sequences Used in q-PCR

Target	Forward (5′-3′) Sequence	Reverse (5′-3′) Sequence
β-actin	GGCTGTATTCCCCTCCATCG	CCAGTTGGTAACAATGCCATGT
IL-1β	GAAATGCCACCTTTTGACAGTG	TGGATGCTCTCATCAGGACAG

Statistical methods

The experimental data were subjected to statistical analysis using GraphPad Prism 8.0 software. The data were presented as mean ± standard deviation (X ± SD). Differences between groups were evaluated using one-way analysis of variance (ANOVA). Statistical significance was represented by $P < 0.05$ (*$P < 0.05$), $P < 0.01$ (**$P < 0.01$), and $P < 0.001$ (***$P < 0.001$), indicating the level of significance of the observed differences.

Bioinformatics Data Analysis Methods

Differentially Expressed Genes (DEGS) in Skin Wounds versus Normal Skin Tissue

The target dataset was downloaded from the GEO database and convert the gene IDs in the two gene expression matrices into the corresponding gene symbols. DEGS screening was then performed after normalization by the limma plug-in package in R language, with the following screening criteria: adjust P value < 0.05; |log2FC|> 1.

Immune Cell Infiltration and Immune-Related Differentially Expressed Genes (Imm-DEGS)

The Cibersort R plug-in package was utilized to analyze the differential infiltration of immune cells in two groups of gene expression matrices: the skin damage group and the normal control group. Immune-related gene sets were downloaded from the ImmPort database, and these gene sets were matched with the DEGS (differentially expressed genes) to identify Imm-DEGS (immune-related differentially expressed genes).

Senescence-Associated Differentially Expressed Genes (Sen-DEGS)

A set of aging-related gene sets was obtained from published findings[40] and then matched to the DEGS (differentially expressed genes) to obtain Sen-DEGS for both the skin wound group and the normal skin group.

PANotosis-Related Differentially Expressed Genes (PAN-DEGS)

Following the approach of previous studies, we selected the PANotosis gene set, which comprises gene sets related to Pyroptosis, Apoptosis, and Necroptosis, from Reactome, AmiGO2, and KEGG databases. Subsequently, this gene set was matched with the DEGS to obtain PAN-DEGS.

GO and GSEA Enrichment Analysis

GO enrichment analysis of DEGS was performed using the clusterprofiler toolkit of R software to understand the biological processes, cellular components, and molecular functions involved in these DEGS. To observe the enrichment of the overall gene expression profile, we analyzed the overall gene expression matrix using the GSEA enrichment method to identify the major expression regulatory pathways involved.

Results

Experimental results

Isolation and Purification of DDNVs

Following various gradients of centrifugation force, the DDNVs were successfully extracted, as illustrated in Figure 2A. Subsequent purification via ultracentrifugation revealed predominant aggregation of plant exosomes in 30%, 45%, and 60% sucrose pads. The purified DDNVs were meticulously collected from the 60% sucrose pads, as depicted in Figure 2B.

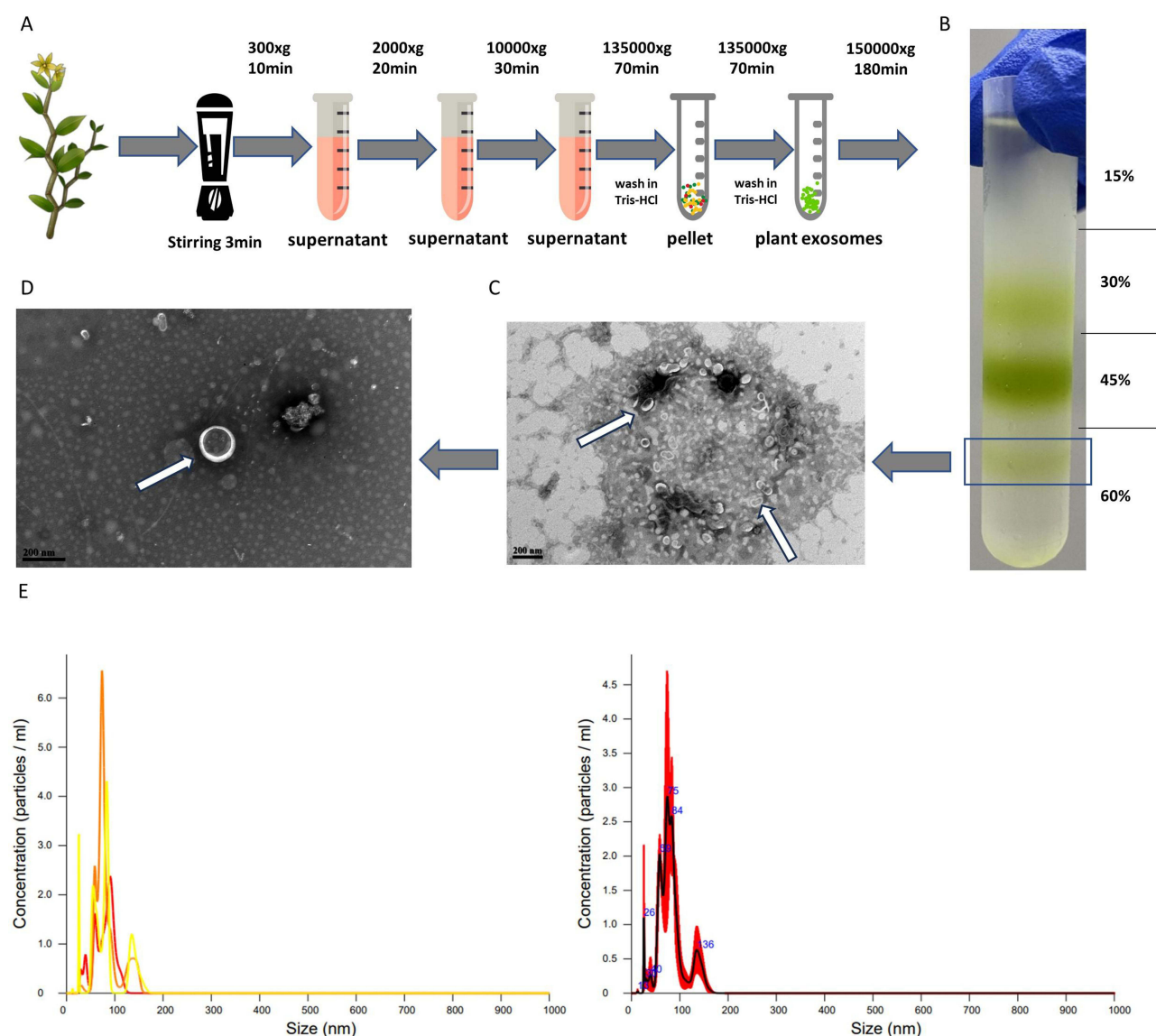**Figure 2** (**A**) Extraction Process of DDNVs. (**B**) Depicts purified exosomes acquired via ultracentrifugation with varying forces and sucrose gradients. (**C** and **D**) As indicated by the white arrows, DDNVs at the 60% lower boundary were observed through transmission electron microscopy. (**E**) Particle size and concentration assessment of DDNVs using NTA detection.

Morphology and Size of DDNVs Observed by Transmission Electron Microscopy

TEM observations of DDNVs in Figure 2C and D revealed uniform morphology in the purified plant nanoparticles. They exhibited a well-defined lipid bilayer membrane structure with a tea tray or hemispherical shape and varied in size (see white arrows). These characteristics align with the typical microscopic identification features of plant nanoparticles.

Determination of DDNVs Particle Size

The NTA analysis of DDNVs demonstrated that the particle size of the purified nanovesicles was predominantly concentrated at 81.9 ± 2.0 nm, with a standard deviation (SD) of 26.6 ± 3.7 nm, as depicted in Figure 2E. The successful purification of DDNVs was confirmed by the narrow and uniform distribution of nanovesicles.

Results of DDNVs Uptake by Skin Tissues

To investigate the in vivo uptake of DDNVs by skin tissues, we injected DIR-labeled DDNVs into the dorsal skin of mice. Within 24 hours post-treatment, we observed the internalization of DDNVs by cells in the dermis layer, as indicated by the white arrows in Figure 3A.
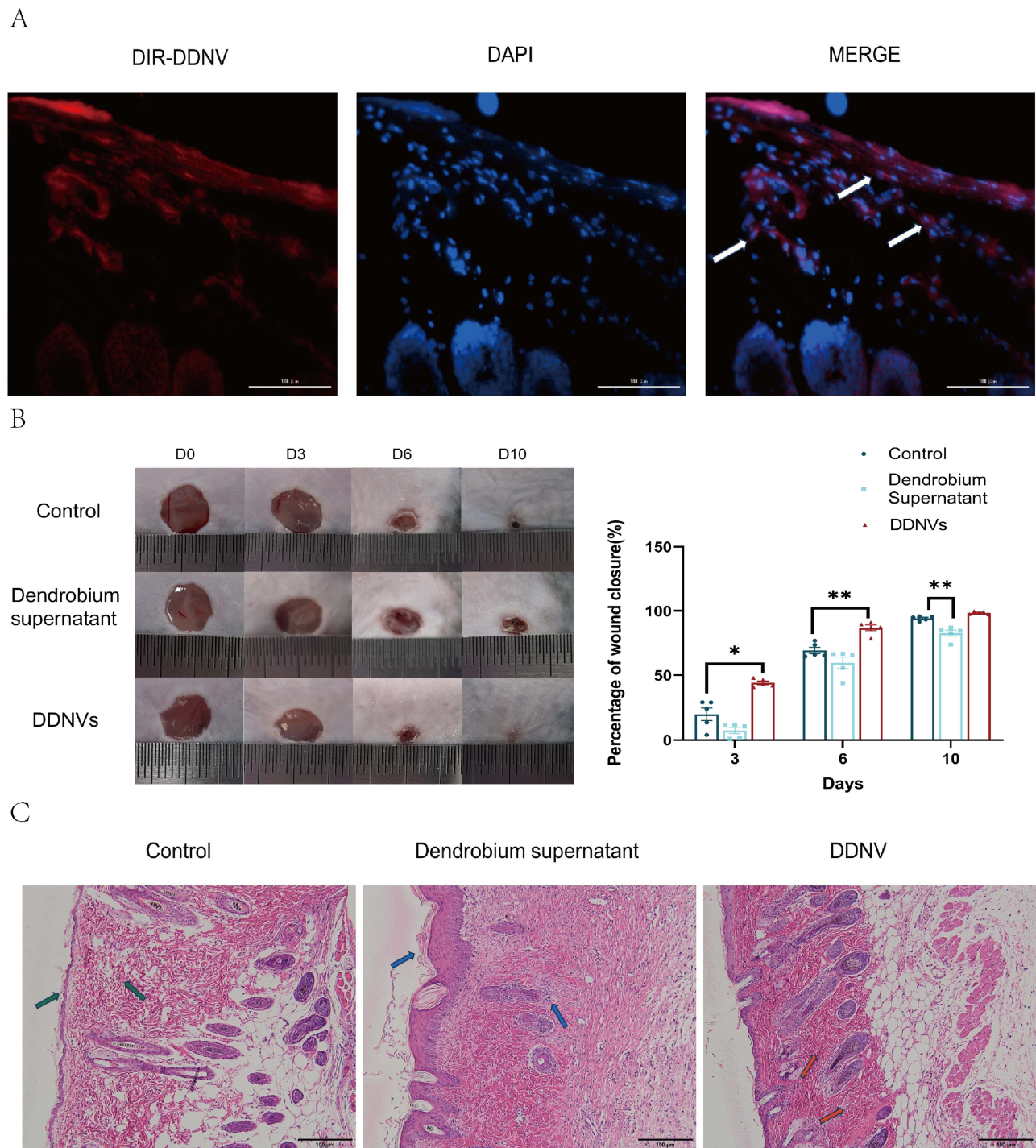
Figure 3 (**A**) Intradermal injection of DIR-labeled DDNVs onto the dorsal skin of C57 mice. After 24 hours, skin tissue was collected. As indicated by the white arrows, DDNVs are internalized by dermal cells. (**B**) Left: Circular full-thickness dermal excision wound on the dorsum of C57 mice. Right: Healing percentage with daily 200 μL (5 mg/mL) DDNVs treatment until wound closure. (**C**) HE staining of mouse skin tissues at 10x magnification. Comparison and observation of HE-stained skin tissue morphology following DDNVs treatment. The control group exhibited epidermal thinning and irregular skin appendages (green arrows). Dendrobium supernatant, lacking exosomes, exhibited epidermal hyperplasia and hyperkeratosis, with an increased presence of inflammatory cells (blue arrows). DDNVs exhibited normal skin appendages, with fewer inflammatory cells (red arrows). Results are from three parallel experiments with consistent outcomes (*p < 0.05, **p < 0.01).

DDNVs Promote Skin Wound Healing

To evaluate the therapeutic potential of DDNVs in skin wound healing, we conducted in vivo experiments using a wound model. The results demonstrated a significant enhancement in cutaneous wound healing in mice treated with DDNVs.

Throughout the 10-day observation period (depicted in Figure 3B), the DDNVs group exhibited markedly improved wound healing at days 0, 3, 6, and 10 compared to the control group. Conversely, wounds treated with the supernatant of *Dendrobium*, with DDNVs removed, did not show significant improvement, suggesting that impurities in the supernatant may have hindered the wound-healing process. By day 10, wounds treated with purified DDNVs in the DDNVs group appeared nearly completely closed.

Hematoxylin and eosin (HE) staining of the skin tissues (Figure 3C) revealed distinct features. The control group exhibited localized thinning of the epidermis and irregular morphology of the skin appendages, indicated by green arrows. In contrast, the *Dendrobium* supernatant group, with the removal of *Dendrobium* exosomes, displayed epidermal hyperplasia and hyperkeratosis, accompanied by a significant accumulation of inflammatory cells denoted by blue arrows. Conversely, the DDNVs group demonstrated normal and intact skin appendages with a reduced presence of inflammatory cells, which were orderly and densely arranged, as indicated by red arrows. These results suggest that DDNVs play a beneficial role in promoting the healing of skin injuries.

Bioinformatics Analysis Results
DEGS in the Skin Wound Group versus the Normal Skin Group
The target gene expression profile was obtained from the GEO database (GSE28914), and six samples from three days after the skin wound and eight samples from normal skin in this microarray were selected for the study. Analysis by the R language limma plug-in package revealed that 1885 genes were highly expressed and 1774 genes were lowly expressed in the skin wound group compared to the normal skin group (see Figure 4A).

Immune Cell Infiltration and Imm-DEGS
The analysis of immune cell infiltration revealed significant differences between the skin wound tissue and normal skin tissue. Specifically, in the skin wound tissue, there was a notable over-infiltration of various immune cell types, including naïve T cells CD4, activated memory CD4 T cells, resting NK cells, monocytes, macrophages M1, macrophages M2, activated dendritic cells, and eosinophils (P values ranging from 0.001 to 0.011). Conversely, the expression status of plasma cells, CD8 T cells, regulatory T cells (Tregs), activated NK cells, resting dendritic cells, and resting mast cells were found to be relatively low (P values ranging from 0.007 to 0.029) (see Figure 4B). Furthermore, we identified 266 Imm-DEGS, of which 204 genes showed high expression in the skin wound group compared to the normal skin group (eg, IL-1β, PTGFR, and VGEFC). On the other hand, 62 genes demonstrated low expression in the skin wound group (eg, IL18, LGR4, VAV3, SDC4, BTC, and AZGP1) (see Figure 4C).

Sen-DEGS
A total of 43 Sen-DEGS were identified, of which 39 Sen-DEGS showed high expression in the skin wound group compared to the normal skin group (eg, CCL5, PECAM1, CCL13, IL1B, CCL2, and PLAU). Additionally, 4 Sen-DEGS demonstrated low expression in the skin wound group (eg, IL18, WNT2, WNT16, and ANG) (see Figure 5A).

Pan-DEGS
We identified a total of 10 DEGS associated with PANotosis. Among them, 8 PAN-DEGS (IRF1, MLKL, GSDMD, AKT3, CD14, LY96, GZMB, IL1B) showed high expression in the skin damage group compared to the normal skin group. On the other hand, 2 genes (IL18 and ELANE) demonstrated low expression in the skin damage group (see Figure 5B).

GO and GSEA Enrichment
Regarding GO enrichment, the DEGS were primarily associated with 2076 biological processes, including leukocyte migration, cell chemotaxis, and myeloid leukocyte migration. They were also linked to 85 cellular components, such as the collagen-containing extracellular matrix and secretory granule membrane, and 66 molecular functions, including cytokine binding and immune receptor activity. Interestingly, individual DEGS were found to be involved in multiple biological pathways; for example, IL-1β was implicated in cell chemotaxis, leukocyte chemotaxis, migration, and myeloid leukocyte migration. Moreover, there were intriguing connections between these biological processes, cellular components, and molecular functions, exemplified by positive regulation of inflammatory response, cellular extravasation, and lipopolysaccharide-binding, as depicted in Figure 6A–D. In terms of GSEA enrichment, the DEGS were prominently associated with
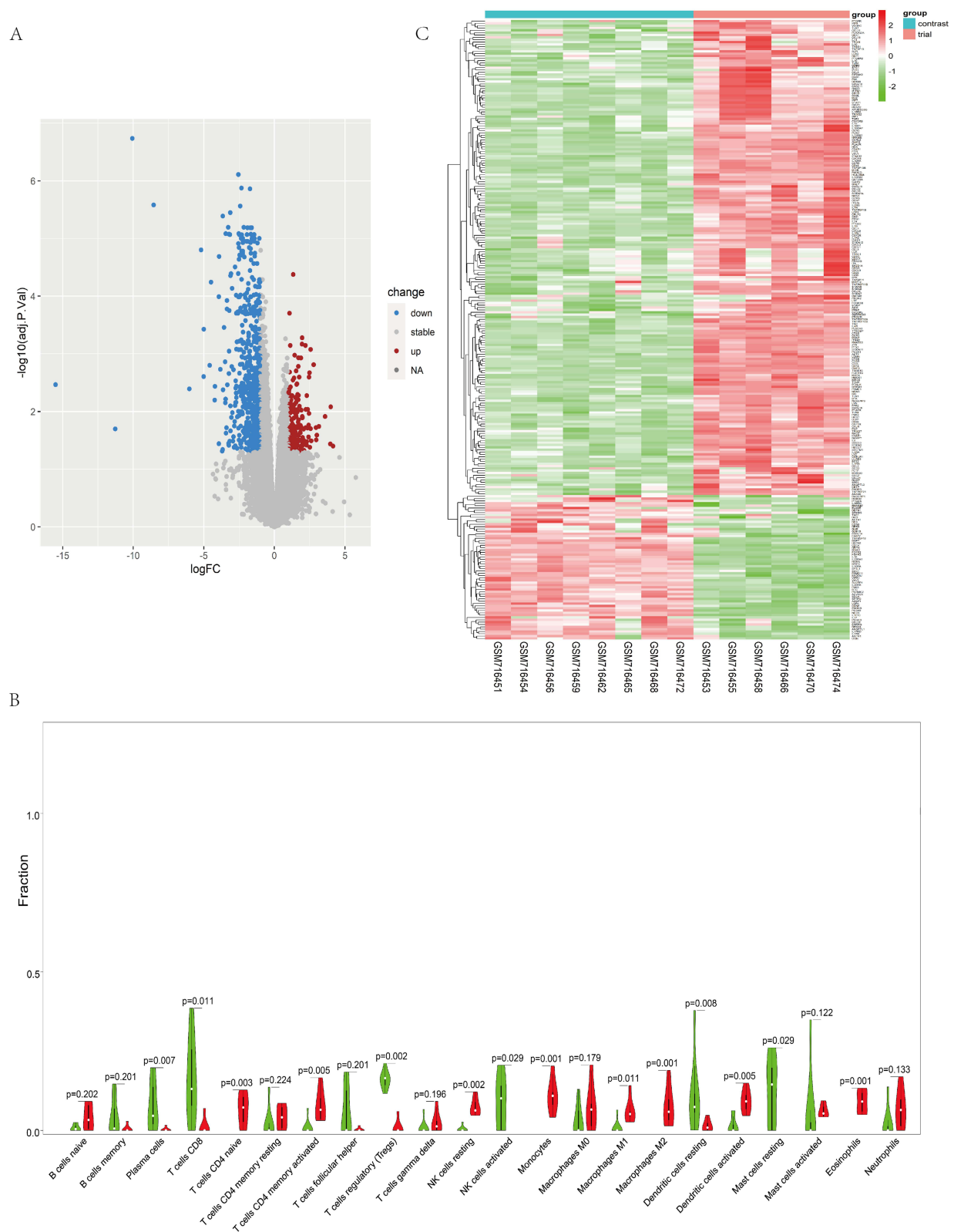
Figure 4 (**A**) Differential Expression of Genes (DEGs): The diagram highlights upregulated DEGs in blue on the left and downregulated DEGs in red on the right. Selection criteria: |logFC| ≥ 1 and adjP ≤ 0.05. (**B**) Analysis of Immune Cell Infiltration: The violin plot presents immune cell infiltration levels in control and experimental groups. Green and red shades represent the proportion of immune cell infiltration. Wilcoxon test p-values reflect. (**C**) Expression Analysis of 266 Immune-DEGs: The graph represents expression levels of 266 Immune-DEGs. Deeper red denotes higher expression, and darker green suggests lower expression. Con group = normal skin tissue; test group = damaged skin tissue.
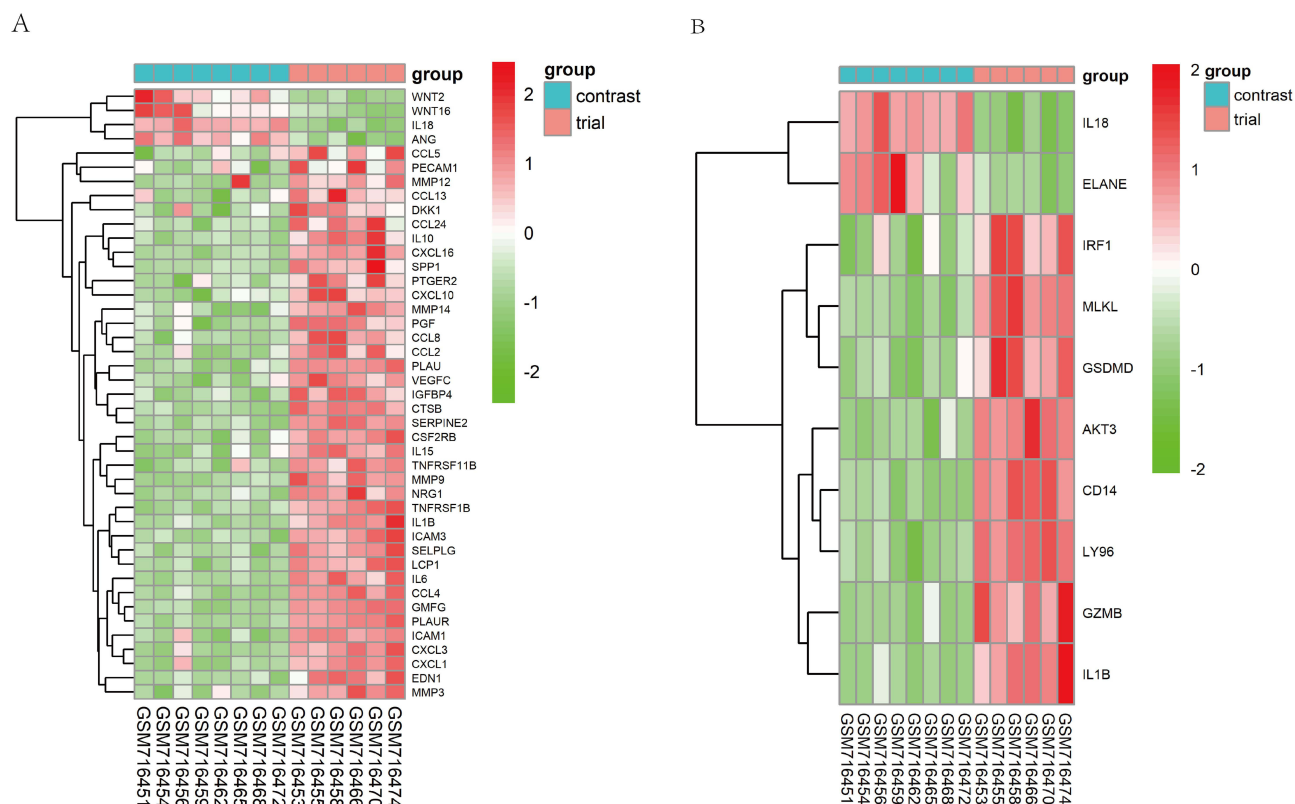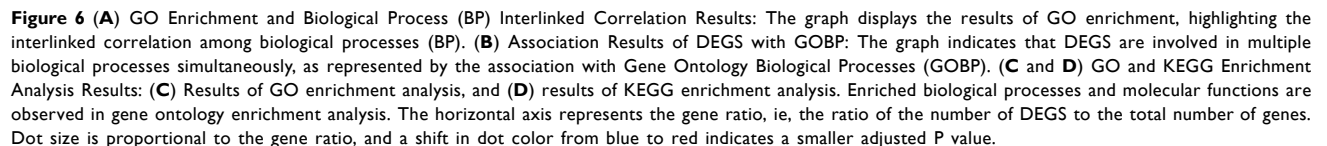
A

B

Figure 5 (**A**) Expression Analysis of 43 Senescence-DEGS: The visualization displays expression levels of 43 Senescence-DEGs. The upper panel's deeper red indicates higher expression, while darker green signifies lower expression. Contrast group = normal skin tissue; test group = damaged skin tissue. (**B**) Expression Profiling of 10 PANoptosis-Associated DEGS: The chart illustrates expression levels of 10 DEGs associated with PANoptosis. Deeper red signifies higher expression, while darker green indicates lower expression. Contrast group = normal skin tissue; test group = damaged skin tissue. The statistical significance of pre- and post-intervention immune cell differences.

pathways such as the IL-17 signaling pathway, NF-kappa B signaling pathway, and Neutrophil extracellular trap formation, as shown in Figure 7A.

Bioinformatics Plus in vivo Validation: Effect of DDNV on IL-1β Expression

Inflammation plays a pivotal role in orchestrating diverse cellular and molecular responses, creating a conducive environment to support epithelialization during the skin wound healing process.[41,42] In acute wound healing, the inflammatory response is activated, leading to vasodilation and increased blood flow to the wound site. This process releases various inflammatory factors, including cytokines, communication molecules, and leukocytes, which coordinate and regulate the healing process by eliminating invading pathogens and foreign bodies[43,44]. However, if the inflammatory response persists, it can hinder the transition from inflammation to re-epithelialization, resulting in challenges in wound healing.[44,45] One key mediator of inflammation is IL-1β, which is activated by soluble factors and produced by monocyte macrophages after contact with stimulated Th1 lymphocytes.[46] In our study, we investigated the skin wound group and found a common highly expressed gene, IL-1β, among Imm-DEGS, Sen-DEGS, and PAN-DEGS (see Figure 7B). To verify the efficacy of DDNVs, we extracted RNA from the skin tissues of mice that had undergone DDNV intervention. The results of qPCR analyses demonstrated that DDNVs effectively inhibited the mRNA expression level of IL-1β (see Figure 7C). Specifically, when compared to the control group, the mRNA expression level of IL-1β was over 2.4-fold higher in the Dendrobium supernatant group with DDNVs removed. In contrast, mice treated with DDNVs showed significant suppression of the mRNA expression level of IL-1β by 2.5-fold, as depicted in Figure 7C.
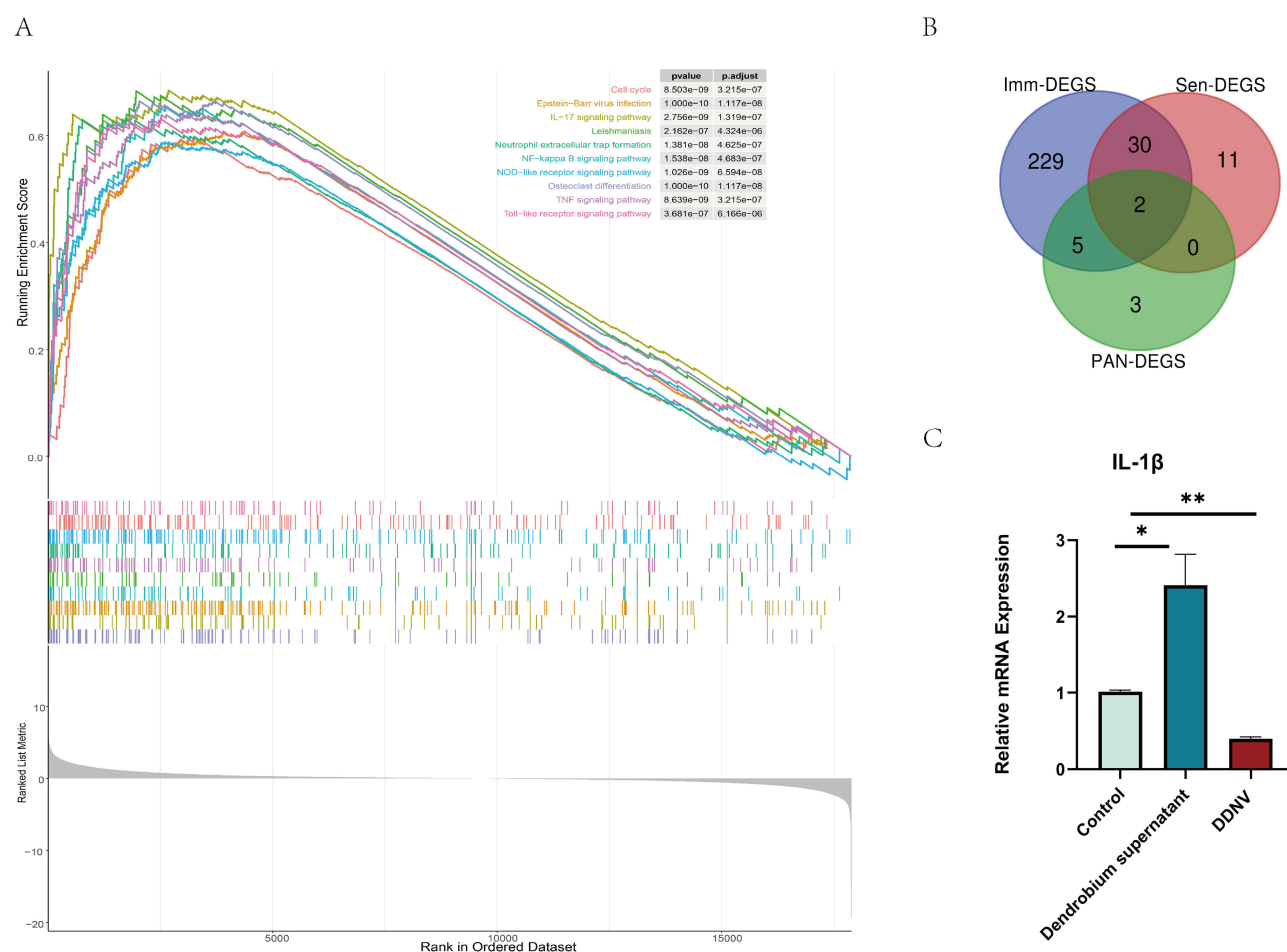
Figure 6 (**A**) GO Enrichment and Biological Process (BP) Interlinked Correlation Results: The graph displays the results of GO enrichment, highlighting the interlinked correlation among biological processes (BP). (**B**) Association Results of DEGS with GOBP: The graph indicates that DEGS are involved in multiple biological processes simultaneously, as represented by the association with Gene Ontology Biological Processes (GOBP). (**C** and **D**) GO and KEGG Enrichment Analysis Results: (**C**) Results of GO enrichment analysis, and (**D**) results of KEGG enrichment analysis. Enriched biological processes and molecular functions are observed in gene ontology enrichment analysis. The horizontal axis represents the gene ratio, ie, the ratio of the number of DEGS to the total number of genes. Dot size is proportional to the gene ratio, and a shift in dot color from blue to red indicates a smaller adjusted P value.

A

	pvalue	p.adjust
Cell cycle	8.503e−09	3.215e−07
Epstein−Barr virus infection	1.000e−10	1.117e−08
IL−17 signaling pathway	2.756e−09	1.319e−07
Leishmaniasis	2.162e−07	4.324e−06
Neutrophil extracellular trap formation	1.381e−08	4.625e−07
NF−kappa B signaling pathway	1.538e−08	4.683e−07
NOD−like receptor signaling pathway	1.026e−09	6.594e−08
Osteoclast differentiation	1.000e−10	1.117e−08
TNF signaling pathway	8.639e−09	3.215e−07
Toll−like receptor signaling pathway	3.681e−07	6.166e−06

B

C

Figure 7 (**A**) Results of GSEA Enrichment Analysis: The graph illustrates GSEA enrichment analysis results, with colored lines representing each pathway. (**B**) Gene Intersection Between Imm-DEGS, Sen-DEGS, and PAN-DEGS: The graph depicts the gene intersection among immune-associated differentially expressed genes (Imm-DEGS), senescence-associated differentially expressed genes (Sen-DEGS), and pan-apoptosis-associated differentially expressed genes (PAN-DEGS). The common genes among the three groups are IL-1β and IL-18. (**C**) The graph displays mRNA expression levels of IL-1β in mouse skin tissues, representing three independent experiments with consistent results. Statistically significant differences are denoted by asterisks (*$p < 0.05$, **$p < 0.01$) compared to the control group. The results demonstrate that DDNVs intervention inhibits IL-1β mRNA expression in the skin wound group, suggesting their potential therapeutic activity in modulating the inflammatory response during wound healing.

Discussion

The medicinal value of natural plants is crucial for human health. Initially, research focused on non-nucleic acid components, but technological advancements now explore genetic-level plant regulation. Despite initial doubts, evidence supports plant-derived exosomes' ability to influence animal diseases, with in vitro studies demonstrating their potential therapeutic applications. In this study, we harnessed ultracentrifugation in conjunction with a four-concentration sucrose-purified water pad to meticulously isolate and purify *Dendrobium* nanovesicles. Subsequently, we conducted a thorough examination of the nanovesicles' morphology, particle size, and bioactivity, validating their association with *Dendrobium* origin. The results, as depicted in Figure 2B–D, substantiate the efficient procurement of purified *Dendrobium* nanovesicles achieved through the synergy of ultracentrifugation and density gradient centrifugation. In vivo investigations on C57 mouse skin tissues revealed successful DDNVs uptake (Figure 3A), holding potential for skin wound tissue regeneration.

In a healthy context, the skin naturally eliminates senescent cells through immune cell efforts. This process involves programmed cell death, immune clearance mechanisms, and the release of "senescence-associated secretory factors" (SASFs).[47] These secreted factors comprise inflammatory chemokines that not only attract but also activate various subpopulations of immune cells, forming a natural barrier to protect the skin tissue.[48] PANoptosis, a precise form of programmed inflammatory cell death,[49,50] regulates immune cells, influencing immune cell infiltration and facilitating

inflammation resolution.[51] A strong correlation exists between PANoptosis, immune infiltration, and cellular senescence, promoting essential processes like cell proliferation, neovascularization, and matrix synthesis, facilitating wound healing.[52]

In this investigation, we made a noteworthy discovery of intersecting genes among aging, immunity, and pan-apoptosis, as depicted in Figure 4F. IL-1β and IL-18 displayed distinct expression patterns, with IL-1β high and IL-18 low in the model group. This observation led us to hypothesize that these two genes may hold significant roles in regulating the repair of skin damage. IL-1β, an interleukin, plays a crucial role as an important regulator in the inflammatory response. It is intricately involved in the immune system, mediating the inflammatory response, and activating immune cells.[53,54] According to the QPCR analysis, it was confirmed that DDNVs effectively suppressed the expression of IL-1β mRNA. In contrast, neither the control group nor the use of *Dendrobium* supernatant with DDNVs removed showed similar inhibition of IL-1β expression. Both DDNVs and DDNVs-removed *Dendrobium* supernatant were filtered with a sterile 0.22 um filter to eliminate bacteria prior to application. Surprisingly, the results from both experiments indicated that the *Dendrobium* supernatant group exhibited even higher IL-1β mRNA expression and slower wound healing than the control group. This observation suggests that the unpurified *Dendrobium* supernatant, with its increased impurity particles, might be applied to broken skin wounds, where the impurities are not easily absorbed, leading to the aggregation of inflammatory cells and adversely affecting the wound repair process. This underscores the importance of purification in obtaining optimal wound-healing outcomes.

Regarding GO and GESA enrichment, our analysis revealed that the differentially expressed genes (DEGs) were predominantly associated with 2076 biological processes, 85 cellular components, and 66 types of molecular functions. The IL-17 signaling pathway, NF-kappa B signaling pathway, and Neutrophil extracellular trap formation (NETosis) played crucial roles in wound repair, connecting with aging, immunity, and pan-apoptosis.[55,56] IL-17 regulates endothelial cell senescence, while inhibiting IL-17A/TNF-α-stimulated human skin fibroblasts promotes skin tissue repair.[57–59] NETosis represents a distinctive form of neutrophil demise,[60] wherein DNA webs and proteins are liberated, ensnaring and eradicating pathogens, thereby actively engaging in immune defense throughout the wound healing process.[61] The IL-17 signaling pathway, NF-κB signaling pathway, NETosis, TNF signaling pathway, and IL-1β intricately intertwine during wound healing.[62–64] The IL-17 signaling pathway and NF-κB signaling pathway synergistically activate downstream molecules, augmenting IL-1β synthesis and release;[65,66] Subsequently, IL-1β release stimulates neutrophils, prompting NETosis formation,[67] Additionally, there is mutual regulation between the TNF signaling pathway and IL-1β, culminating in the co-activation of the inflammatory response and apoptosis,[66] fostering the regeneration of skin tissues. DDNVs modulate IL-1β, suppressing inflammatory responses and potentially inducing the IL-17 signaling pathway activation. They indirectly regulate the NF-κB signaling pathway, NETosis, and TNF signaling pathway to modulate apoptosis, cellular senescence, immune infiltration, and promote cellular proliferation during wound healing. As a natural therapeutic agent, DDNVs have the potential to regulate multiple critical signaling pathways, fostering effective wound healing.

Conclusions

In this study, we isolated and purified DDNVs and confirmed the potential of DDNVs to promote skin wound healing in C57 mice. Bioinformatics identified IL-1β as pivotal in skin tissues, immune infiltration, aging, and pan-regulatory demise. DGES analysis suggested DDNVs may be involved in diverse biological processes and molecular functions, emphasizing potential mechanisms like IL-17, NF-κB, NETosis, and TNF pathways. These, closely linked to IL-1β, collectively regulate cellular senescence, immune infiltration, and wound healing. This provides new strategies and targets for future understanding of cellular senescence, apoptosis, and immune infiltration in skin wound repair.

Abbreviations

DDNVs, *Dendrobium*-derived nanovesicles; PDNV, plant-derived nanovesicles; GOBP, Gene Ontology Biological Processes; DEG, differentially expressed genes; Imm-DEGS, immune-related differentially expressed genes; PAN-DEGS, PANotosis-related differentially expressed genes; Sen-DEGS, Senescence-associated differentially expressed genes; TEM, Transmission electron microscopy; BP, Biological Process.

Data Sharing Statement

All the data in the study are available upon reasonable request from the corresponding authors.

Acknowledgments

Author Contributions

All authors made a significant contribution to the work reported, whether that is in the conception, study design, execution, acquisition of data, analysis and interpretation, or in all these areas; took part in drafting, revising or critically reviewing the article; gave final approval of the version to be published; have agreed on the journal to which the article has been submitted; and agree to be accountable for all aspects of the work.

Funding

Disclosure

The authors declare that they have no known competing financial interests or personal relationships that could have appeared to influence the work reported in this paper.

References

1. Zhiheng H, Ong CH, Jaroslava H, Andrew B. Progranulin is a mediator of the wound response. *Nature Med*. 2003;9(2):225–229.
2. Garraud O, Hozzein WN, Badr G. Wound healing: time to look for intelligent, "natural" immunological approaches? *BMC Immunol*. 2017;18(Suppl 1):1–8.
3. Kamila R, Yevgeniy K, Zharylkasyn Z, Kuat K, Shiro J, Arman S. Immunology of acute and chronic wound healing. *Biomolecules*. 2021;11(5):700.
4. Graves N, Phillips CJ, Harding K. A narrative review of the epidemiology and economics of chronic wounds. *Br j dermatol*. 2021;187(2):141–148.
5. Rodrigues M, Kosaric N, Bonham CA, Gurtner GC. Wound healing: a cellular perspective. *Physiol Rev*. 2019;99(1):665–706.
6. Yağız S, Kaan KO, Turhan BB, et al. Grapefruit-derived extracellular vesicles as a promising cell-free therapeutic tool for wound healing. *Food Funct*. 2021;12:5144–5156.
7. Science; Researchers at Hangzhou Normal University Release New Data on Science. A transcriptome-wide, organ-specific regulatory map of Dendrobium officinale, an important traditional Chinese orchid herb. *Sci Letter*. 2017;6(1):18864.
8. Hanxiao T, Tianwen Z, Yunjie S, Ting Z, Lingzhu F, Yongsheng Z. Dendrobium officinale Kimura et Migo: a review on its ethnopharmacology, phytochemistry, pharmacology, and industrialization. *Evid Based Complement Alternat Med*. 2017. doi:10.1155/2017/7436259
9. Zhicai W, Meili Z, Hongqiu C, Jian L, Meina W. Transcriptomic landscape of medicinal dendrobium reveals genes associated with the biosynthesis of bioactive components. *Front Plant Sci*. 2020;11:391.
10. Hu WY. Traditional uses, chemical constituents, pharmacological activities, and toxicological effects of Dendrobium leaves: a review. *J Ethnopharmacol*. 2021;270:113851.
11. Aleksandra B, Magdalena N, Magdalena D, Szlachetko DL. Micromorphology of Labellum in selected Dendrobium Sw. (Orchidaceae, Dendrobieae). *Int J Mol Sci*. 2022;23(17):9578.
12. Zuo S-M, Yu H-D, Zhang W, et al. Comparative metabolomic analysis of dendrobium officinale under different cultivation substrates. *Metabolites*. 2020;10(8):325. doi:10.3390/metabo10080325
13. Wei L, Xingrui M, Xingqian W, et al.; Dendrobium nobile Lindl. Polysaccharides protect fibroblasts against UVA-induced photoaging via JNK/c-Jun/MMPs pathway. *J Ethnopharmacol*. 2022;298:115590.
14. Sooyeon H, EunYoung K, SeoEun L, JaeHyun K, Youngjoo S, HyukSang J. Dendrobium nobile Lindley administration attenuates atopic dermatitis-like lesions by modulating immune cells. *Int J Mol Sci*. 2022;23(8):9578.
15. Yin XB, Qu CH, Dong XX, Shen MR, Ni J. 《中国药典》2020年版一部收录中成药制法规律分析 [Preparation regularity of Chinese patent medicine in Chinese Pharmacopoeia (2020 edition, Vol. I)]. *Zhongguo Zhong yao za zhi*. 2022;47(16):4529–4535. Chinese.
16. Jian C, Hui Q, Jin-Biao L, et al. 铁皮石斛多糖促进毛发生长的实验研究 [Experimental study on Dendrobium candidum polysaccharides on promotion of hair growth]. *Zhongguo Zhong yao za zhi*. 2014;39(2):291–295. Chinese.
17. Xin Z, Peng S, Yu Q, Huayi SD. candidum has in vitro anticancer effects in HCT-116 cancer cells and exerts in vivo anti-metastatic effects in mice. *Nutr Res Pract*. 2014;8(5):487–493.
18. Teixeira da Silva JA, Tsavkelova EA, Zeng S, et al. Symbiotic in vitro seed propagation of Dendrobium: fungal and bacterial partners and their influence on plant growth and development. *Planta*. 2015;242(1):1–22.
19. Mengmeng W, Erwei Z, Chenrui Y, et al. Dendrobium officinale enzyme changing the structure and behaviors of Chitosan/γ-poly(glutamic acid. *Hydrogel Potent Skin Care Polymers*. 2022;14(10):2070.
20. Anesh P, Jay JW, Daniel J, Wolf SE, El Amina A. Role of exosomes in dermal wound healing: a systematic review. *J invest dermatol*. 2021;142 (3PA):662–678.

21. Mengdie L, Tao W, He T, Guohua W, Liang Z, Yijie S. Macrophage-derived exosomes accelerate wound healing through their anti-inflammation effects in a diabetic rat model. *Artif Cells Nanomed Biotechnol*. 2019;47(1):3793–3803.

22. Li X, Liu L, Yang J, et al. Exosome derived from human umbilical cord mesenchymal stem cell mediates MiR-181c attenuating burn-induced excessive inflammation. *EBioMedicine*. 2016;8(C):72–82. doi:10.1016/j.ebiom.2016.04.030

23. Shi Z, Wang Q, Jiang D. Extracellular vesicles from bone marrow-derived multipotent mesenchymal stromal cells regulate inflammation and enhance tendon healing. *J Transl Med*. 2019;17(1). doi:10.1186/s12967-019-1960-x

24. Juan X, Suwen B, Yadi C, et al. miRNA-221-3p in endothelial progenitor cell-derived exosomes accelerates skin wound healing in diabetic mice. *Diabetes Metabol Syndr Obes*. 2020;13:1259–1270.

25. Jieyuan Z, Chunyuan C, Bin H, et al. Exosomes derived from human endothelial progenitor cells accelerate cutaneous wound healing by promoting angiogenesis through Erk1/2 signaling. *Int J Bio Sci*. 2016;12(12):1472.

26. Bin Z, Xiaodong L, Xiaomin S, et al. Exosomal MicroRNAs derived from human amniotic epithelial cells accelerate wound healing by promoting the proliferation and migration of fibroblasts. *Stem Cells Int*. 2018;2018:2018.

27. Tao M, Bingchuan F, Xin Y, Yilei X, Mengxiong P, Tao M. Adipose mesenchymal stem cell-derived exosomes promote cell proliferation, migration, and inhibit cell apoptosis via Wnt/β-catenin signaling in cutaneous wound healing. *J Cell Biochem*. 2019;120(6):19496–19508. doi:10.1002/jcb.29253

28. XueHan X, TieJun Y, Anwar DH, et al. Plant exosomes as novel nanoplatforms for MicroRNA transfer stimulate neural differentiation of stem cells in vitro and in vivo. *Nano Lett*. 2021.8151–8159.

29. Qilong W, Xiaoying Z, Jingyao M, et al. Delivery of therapeutic agents by nanoparticles made of grapefruit-derived lipids. *Nat Commun*. 2013;4(1):1867.

30. Peng L-H, Wang M-Z, Chu Y, et al. Engineering bacterial outer membrane vesicles as transdermal nanoplatforms for photo-TRAIL–programmed therapy against melanoma. *Sci Adv*. 2020;6(27). doi:10.1126/sciadv.aba2735

31. Song Y, Shuyan L, Limei R, et al. Ginseng-derived nanoparticles induce skin cell proliferation and promote wound healing. *J Ginseng Res*. 2023;47(1):1867.

32. Fikrettin Ş, Polen K, Yıldırım GM, Irem Ö, Ezgi Y, Yağmur KE. In vitro wound healing activity of wheat-derived nanovesicles. *Appl Biochem Biotechnol*. 2018;188(2):381–394.

33. Manho K, Hyun PJ. Isolation of aloe saponaria-derived extracellular vesicles and investigation of their potential for chronic wound healing. *Pharmaceutics*. 2022;14(9):1905.

34. Shilo S, Roth S, Amzel T, et al. Cutaneous wound healing after treatment with plant-derived human recombinant collagen flowable gel. *Tissue Eng Part A*. 2013;19(13–14):1519–1526. doi:10.1089/ten.TEA.2012.0345

35. Wynn TA, Vannella KM. Macrophages in tissue repair, regeneration, and fibrosis. *Immunity*. 2016;44(3):450–462. doi:10.1016/j.immuni.2016.02.015

36. Franceschi C, Garagnani P, Vitale G, Capri M, Salvioli S. Inflammaging and 'Garb-aging. *Trends Endocrinol Metab*. 2016;28(3):199–212.

37. Tottoli EM, Dorati R, Genta I, Chiesa E, Pisani S, Conti B. Skin wound healing process and new emerging technologies for skin wound care and regeneration. *Pharmaceutics*. 2020;12(8):735. doi:10.3390/pharmaceutics12080735

38. Ellis S, Lin EJ, Tartar D. Immunology of wound healing. *Curr Dermatol Rep*. 2018;7(4):350–358.

39. Kun W, Yuwen L, Tiantian Z, et al. Overexpression of c-Met in bone marrow mesenchymal stem cells improves their effectiveness in homing and repair of acute liver failure. *Stem Cell Res Ther*. 2017;8(1):1.

40. Saul D, Kosinsky RL, Atkinson EJ, et al. A new gene set identifies senescent cells and predicts senescence-associated pathways across tissues. *Nat Commun*. 2022;13(1):4827.

41. Koh TJ, DiPietro LA. Inflammation and wound healing: the role of the macrophage. *Expert Rev Mol Med*. 2011;13. doi:10.1017/S1462399411001943

42. Shukla SK, Sharma AK, Gupta V, Yashavarddhan MH. Pharmacological control of inflammation in wound healing. *J Tissue Viabil*. 2019;28(4):218–222. doi:10.1016/j.jtv.2019.09.002

43. Nowak NC, Menichella DM, Miller R, Paller AS. Cutaneous innervation in impaired diabetic wound healing. *Transl Res*. 2021;236:87–108.

44. Xu LN, Dongqing L, Mona S. Transition from inflammation to proliferation: a critical step during wound healing. *Cell Mol Life Sci*. 2016;73(20):3861–3885.

45. Zhao R, Liang H, Clarke E, Jackson C, Xue M. Inflammation in chronic wounds. *Int J Mol Sci*. 2016;17(12):2085.

46. Barrientos S, Stojadinovic O, Golinko MS, Brem H, Tomic-Canic M. Growth factors and cytokines in wound healing. *Wound Repair Regener*. 2008;16(5):585–601.

47. Burton DG, Faragher RG. Cellular senescence: from growth arrest to immunogenic conversion. *Age*. 2015;37(2):1–9.

48. Carlos AJ, Ana B, Torsten W, et al. A complex secretory program orchestrated by the inflammasome controls paracrine senescence. *Nat Cell Biol*. 2013;15(8):978–990.

49. Adi S, Valery K. Immunosurveillance of senescent cells: the bright side of the senescence program. *Biogerontology*. 2013;14(6):617–628.

50. Dan Y, Yue X, Yuxun S, et al. Anti-PANoptosis is involved in neuroprotective effects of melatonin in acute ocular hypertension model. *J Pineal Res*. 2022;73(4):e12828.

51. Sarhan J, Liu BC, Muendlein HI, et al. Caspase-8 induces cleavage of gasdermin D to elicit pyroptosis during Yersinia infection. *Proc Natl Acad Sci USA*. 2018;115(46):E10888–E10897.

52. Nagakannan P, ThirumalaDevi K. PANoptosis: a unique innate immune inflammatory cell death modality. *J Iimmunol*. 2022;209(9):1625–1633.

53. Okizaki S-I, Ito Y, Hosono K, et al. Vascular endothelial growth factor receptor type 1 signaling prevents delayed wound healing in diabetes by attenuating the production of IL-1β by Recruited macrophages. *Am J Pathol*. 2016;186(6):1481–1498. doi:10.1016/j.ajpath.2016.02.014

54. Nanako K, Rei N, Kanae S, et al. Interleukin-1β promotes interleulin-6 expression via ERK1/2 signaling pathway in canine dermal fibroblasts. *PLoS One*. 2019;14(7):e0220262.

55. Malak A, Laurence J, Cyril A, et al. Endothelial microparticles from acute coronary syndrome patients induce premature coronary artery endothelial cell aging and thrombogenicity: role of the Ang II/AT1 Receptor/NADPH oxidase-mediated activation of MAPKs and PI3-Kinase pathways. *Circulation*. 2017;135(3):280–296.

56. Delphine G, Estela B, Christine T, et al. NET formation in bullous pemphigoid patients with relapse is modulated by IL-17 and IL-23 interplay. *Front Immunol*. 2019;10:701.

57. Liang Z, Manli L, Wenhua L, et al. Th17/IL-17 induces endothelial cell senescence via activation of NF-κB/p53/Rb signaling pathway. *Lab Invest*. 2021;101(11):1418–1426.

58. Paloma S, Elisabetta M, Júlia B, et al. Targeting lymphoid-derived IL-17 signaling to delay skin aging. *Nature Aging*. 2023;3(6):1–7.

59. Yin L, Hu Y, Xu J, Guo J, Tu J, Yin Z. Ultraviolet B Inhibits IL-17A/TNF-α-stimulated activation of human dermal fibroblasts by decreasing the expression of IL-17RA and IL-17RC on fibroblasts. *Front Immunol*. 2017;8:91.

60. Mistry P, Carmona-Rivera C, Ombrello AK, et al. Dysregulated neutrophil responses and neutrophil extracellular trap formation and degradation in PAPA syndrome. *Ann Rheumatic Dis*. 2018;77(12):1825–1833.

61. Pedersen F, Waschki B, Marwitz S, et al. Neutrophil extracellular trap formation is regulated by CXCR2 in COPD neutrophils. *Europ resp J*. 2018;51(4):1700970. doi:10.1183/13993003.00970-2017

62. Ménoret A, Buturla JA, Xu MM, et al. T cell-directed IL-17 production by lung granular γδ T cells is coordinated by a novel IL-2 and IL-1β circuit. *Mucosal Immunol*. 2018;11(5):1398–1407. doi:10.1038/s41385-018-0037-0

63. Kamran G, Anna B, Charlotta E, Robert S. Therapeutics targeting the IL-23 and IL-17 pathway in psoriasis. *Lancet*. 2021;397(10275):754–766.

64. Monteleone NJ, Lutz CS, Fioravanti A. miR-708 negatively regulates TNFα/IL-1β signaling by suppressing NF-κB and arachidonic acid pathways. *Mediat Inflammat*. 2021;2021:5595520. doi:10.1155/2021/5595520

65. Cai Y, Xue F, Quan C, et al. A critical role of the IL-1β-IL-1R signaling pathway in skin inflammation and psoriasis pathogenesis. *J Invest Dermatol*. 2018;139(1):146–156. doi:10.1016/j.jid.2018.07.025

66. Gendrisch F, Esser PR, Schempp CM, Wölfle U. Luteolin as a modulator of skin aging and inflammation. *Bio Factors*. 2020;47(2):170–180.

67. Shuainan Z, Ying Y, Yun R, et al. The emerging roles of neutrophil extracellular traps in wound healing. *Cell Death Dis*. 2021;12(11):984.